Journal of Clinical and Translational Hepatology **2023**
DOI: 10.14218/JCTH.2023.00019

Original Article

Establishment and Validation of a Four-stress Granule-related Gene Signature in Hepatocellular Carcinoma

Mengzhu Li[1,2,3,4], Xiude Fan[2,3,4], Jiajun Zhao[2,3,4*] and Dawei Wang[1,2,3,4*]

[1]Department of Endocrinology, Shandong Provincial Hospital, Shandong University, Jinan, Shandong, China; [2]Key Laboratory of Endocrine Glucose & Lipids Metabolism and Brain Aging, Ministry of Education; Department of Endocrinology, Shandong Provincial Hospital Affiliated to Shandong First Medical University, Jinan, Shandong, China; [3]Shandong Key Laboratory of Endocrinology and Lipid Metabolism, Jinan, Shandong, China; [4]Shandong Institute of Endocrine and Metabolic Diseases, Jinan, Shandong, China

Received: 26 January 2023 | **Revised:** 17 May 2023 | **Accepted:** 5 June 2023 | **Published online:** 25 July 2023

Abstract

Background and Aims: Stress granules (SGs) as membrane-less cytoplasmic foci formed in response to unfavorable external stimuli could promote cancer cells to adapt to hostile environments. Hepatocellular carcinoma (HCC) is prone to be highly aggressive once diagnosed, which markedly reduces patient survival time. Therefore, it is crucial to develop valid diagnostic markers to prognosticate HCC patient prognosis, which promotes individualized precision therapeutics in HCC. Considering the pro-tumorigenic activity of SGs, it is of great potential value to construct a prognostic tool for HCC based on the expression profiles of SG-related genes (SGGs). ***Methods:*** Bioinformatic analysis was employed to establish an SGG-based prognostic signature. Western blotting and real-time polymerase chain reaction assays were used to assess the expression patterns of the related SGGs. Loss-of-function experiments were performed to analyze the effect of the SGGs on SG formation and cell survival. ***Results:*** A four-SGG signature (*KPNA2*, *MEX3A*, *WDR62*, and *SFN*) targeting HCC was established and validated to exhibit a robust performance in predicting HCC prognosis. Consistently, all four genes were further found to be highly expressed in human HCC tissues. More important, we demonstrated that individually knocking down the four SGGs significantly reduced HCC cell proliferation and metastasis by compromising the SG formation process. ***Conclusions:*** We developed an SGG-based predictive signature that can be used as an independent prognostic tool for HCC. The strong predictive power of this signature was further elucidated by the carcinogenic activity of *KPNA2*, *MEX3A*, *WDR62*, and *SFN* in HCC cells by regulating SG formation.

Citation of this article: Li M, Fan X, Zhao J, Wang D. Establishment and Validation of a Four-stress Granule-related Gene Signature in Hepatocellular Carcinoma. J Clin Transl Hepatol 2023. doi: 10.14218/JCTH.2023.00019.

Introduction

Stress granules (SGs) are membrane-less cytoplasmic foci comprising mRNA, RNA-binding proteins, ribosomal subunits, and eukaryotic translation initiation factors.[1] When eukaryotic cells are subjected to various environmental stimuli like hypoxia, acidosis, oxidative stress, and virus infection, SG formation attenuates protein synthesis to save energy, therefore this process is widely accepted to be a self-protective mechanism for cell survival.[2] Notably, hypoxia, acidosis, and reactive oxygen species characterize the tumor microenvironment.[3] By the formation of SGs, cancer cells could adapt to those hostile nonphysiological conditions for maintaining their continuous growth.[4] Recently, increasing evidence indicates that SGs are closely related to cancer proliferation, metastasis, and chemotherapy.[5] Thus, targeting SGs is considered a promising approach for cancer treatment.

To date, through SG enrichment and proteomic analysis, more than 400 SG-related proteins have been identified.[6] It has been reported that the overexpression of some core SG proteins alone, for example, G3BP1, could induce SG formation even without stress conditions.[7] As the key regulator of SG assembly, G3BP1 is upregulated in various cancers, like prostate, lung, and breast cancers.[8] It is elucidated that the enhancement of G3BP1 translation induces SG formation, resulting in sarcoma metastasis and invasion.[9] Along with this line, it is expected that when G3BP1 is knocked out, SGs would disassemble, accompanied by reduced sarcoma metastasis and invasion.[10]

Keywords: Hepatocellular carcinoma; Stress granules; Prognostic factor; G3BP1.

Abbreviations: AUC, area under the curve; BCA, bicinchoninic acid; BRCA, breast cancer; CCK, cell counting kit; EdU, 5-ethynyl-2-deoxyuridine; G3BP1, ras GTPase-activating protein-binding protein 1; GEO, gene expression omnibus; GO, gene ontology; GSEA, gene set enrichment analysis; HBV, hepatitis B virus; HCC, hepatocellular carcinoma; HCV, hepatitis C virus; HRP, horseradish peroxidase; HRs, hazard ratios; ICGC, international cancer genome consortium; IF, immunofluorescence; KEGG, kyoto encyclopedia of genes and genomes; KIRC, kidney renal clear cell carcinoma; LIHC, human liver hepatocellular carcinoma; LUAD, lung adenocarcinoma; LUSC, lung squamous cell carcinoma; MSGP, mammalian stress granules proteome; N/A, not available; NAFLD, nonalcoholic fatty liver disease; OS, overall survival; OV, ovarian cancer; PPI, protein-protein interaction; PRAD, prostate adenocarcinoma; PVDF, polyvinylidene difluoride; qPCR, quantitative real-time polymerase chain reaction; ROC, receiver operating characteristic; ROS, reactive oxygen species; RBPs, RNA-binding proteins; SDS-PAGE, sodium dodecyl-sulfate polyacrylamide gel electrophoresis; SGs, stress granules; SGGs, stress granule genes; TCGA, the cancer genome atlas; WB, western blot.

***Correspondence to:** Dawei Wang and Jiajun Zhao, Department of Endocrinology, Shandong Provincial Hospital Affiliated to Shandong First Medical University, Jinan, Shandong 250000, China. ORCID: https://orcid.org/0000-0001-7902-001X (DW) and https://orcid.org/0000-0003-3267-9292 (JZ). Tel: +86-531-68776094, Fax: +86-531-87068707, E-mail: wdwdelight@hotmail.com (DW) and jjzhao@sdu.edu.cn (JZ)

As the most prevalent primary malignant liver tumor, hepatocellular carcinoma (HCC) is often diagnosed at a late stage in light of its insidious onset, which prevents patients from receiving radical treatment.[11,12] Even worse, the treatment methods available at this stage are only effective in a few patients.[13] However, if HCC is diagnosed in the early stage, there are more effective curative treatment options. It is thus vital to develop a tool for the early prognosis of HCC patients.[14,15] The current predictive model relies on histopathological characteristics and cancer staging, which does not accurately predict the clinical outcome of early-stage patients.[16] Therefore, it is essential to find one or more sensitive and specific prognostic indicators to detect HCC patients at the occurrence stage, guiding just-in-time therapeutic interventions to improve survival outcomes.

Recently, several gene signatures based on specific cell activities, such as autophagy and ferroptosis, have provided an early and good prognosis for individuals with HCC.[17,18] As SG assembly promotes tumorigenesis through regulation of gene expression regulation and signal transduction,[5,19] stress granule genes (SGGs) might be a potential target for early HCC detection. However, no studies have considered SGGs for predicting HCC patient clinical outcomes. It would be interesting to investigate whether SGGs could be used to construct a predictive gene panel to independently predict HCC development, which mutually compensates with other clinical characteristics.

Methods

Data

The International Cancer Genome Consortium (ICGC; https://dcc.icgc.org/) and The Cancer Genome Atlas (TCGA; https://portal.gdc.cancer.gov/) databases provided the gene expression and clinical data used in this study. Gene expression data of GSE36376, GSE14520, GSE10143, GSE54236, and GSE76427 were collected from the Gene Expression Omnibus (GEO) database (https://www.ncbi.nlm.nih.gov/geo/); gene expression information of CHCC-HBV was from published research.[20] Etiological information and baseline clinical characteristics of HCC patients that were available in the TCGA/GSE/CHCC-HBV/ICGC databases are summarized in Supplementary Tables 1 and 2, and 463 mammalian SGGs were retrieved from the Mammalian Stress Granules Proteome (MSGP) database (https://msgp.pt).

Differential expression and functional enrichment of SGGs

The analysis of the differentially expressed SGGs between healthy and HCC liver tissue from TCGA cohorts was conducted in R. The cutoffs were: |log2 fold-change (FC)|>2 and adjusted *p*-value <0.05. GEO2R (https://www.ncbi.nlm.nih.gov/geo/geo2r/) was employed in evaluating the differential expression of SGGs in normal liver and HCC tissue from GEO cohorts following the criteria of |log2 (FC)|>0.6 and adjusted *p*-value <0.05. KEGG, GO, and GSEA analysis were applied as previously described.[21]

Prognostic risk model development

To identify the prognostic risk signature based on SGGs, univariate and multivariate Cox proportional hazards regression analyses were performed in R using the survival package. Patient risk scores were calculated as:

$$\sum_{i=1}^{n} \text{Coef i} \times \text{EXP gene(i)}$$

where Coef i stands for gene (i)'s Cox regression coefficient, and EXP gene (i) is the expression level of gene i. A median risk score was used as the cutoff to divide HCC patients into low- and high-risk score groups. Survival was described by the Kaplan-Meier method and log-rank analysis. Model sensitivity and specificity were evaluated by receiver operating characteristic (ROC) curve analysis.

HCC samples and cell lines

HCC samples and para-tumor tissues with pathology confirmation were collected from HCC patients at Shandong Provincial Hospital Affiliated to Shandong First Medical University (Jinan, China) between the years 2021 and 2022. All experiments were approved and supervised by the Hospital's Medical Ethics Committee and followed the latest version of the Declaration of Helsinki. Informed consent was obtained from all participants. Hep3B, Huh-7, HepG2, SK-Hep1, PLC, and L-02 cell lines from ATCC (https://www.atcc.org/) were cultured according to the manufacturing instructions. The specified lentivirus was introduced into Hep3B cells or Huh-7 cells followed by puromycin or blasticidin selection.

Plasmids and lentivirus preparation

Lentiviral constructs expressing short hairpin RNA (shRNA) against human *KPNA2*, *MEX3A*, *WDR62*, and *SFN* were purchased from Hedgehogbio (Shanghai, China). shG3BP1 lentiviral plasmid was acquired from Genechem (Shanghai, China). The human *G3BP1* overexpression construct was generated by inserting the human *G3BP1* sequence into the pLV3-CMV-EGFP backbone. Lentiviral particles were generated by transfecting target constructs, packaging, and enveloping plasmids into HEK293T cells; 48h later, the supernatants were collected and filtered utilizing 0.22 μm filters. All shRNA target sequences are placed in Supplementary Table 3.

RNA extraction and qPCR

Total RNA was isolated by TRIzol Reagents (#15596026; ThermoFisher Scientific, Waltham, MA, USA) as previously described.[22] cDNA was synthesized with PrimeScript RT reagent kits (#RR047A; Takara, Shiga, Japan). Target gene expression was quantified by the $2^{-\Delta\Delta Ct}$ method. Supplementary Table 4 includes the primer sequences.

Western blotting

RIPA buffer (#P0013B; Beyotime, Beijing, China) was used to prepare protein samples. Protein concentration was determined with a bicinchoninic acid (BCA) assay kit (BCA Kit, #K3001; Shenergy Biocolor, Shanghai, China), the normalized protein samples were separated by sodium dodecyl-sulfate polyacrylamide gel electrophoresis (SDS-PAGE) and transferred into the polyvinylidene difluoride (PVDF) membranes. After blocking with 5% milk, the membranes were incubated with primary antibodies overnight followed by incubation with horseradish peroxidase (HRP)-conjugated secondary antibodies. Supplementary Table 5 lists the primary antibodies.

Cell counting kit (CCK)8 assay

Cells were planted in a 96-well plate for 24 h at 1×10^4 cells per well, and 10 μL CCK8 (#CK04; Dojindo Laboratories, Kumamoto, Japan) was added to the culture medium for 90 m at the indicated time. Cell absorbance was measured at 450 nm.

Colony formation assay

A population of 250 cells was seeded per well in a 24-well

plate. After 10 days of culture, the cells were fixed with 4% paraformaldehyde before staining with 0.1% crystal violet. Cell clones were photographed before statistical analysis.

5-ethynyl-2-deoxyuridine (EdU) staining assay

Cells were planted in a 96-well plate for 24 h at 1×10^4 cells per well and the EdU staining assay was performed following the kit manufacturer's instructions. (#C10310; RiboBio, Guangzhou, Guangdong, China). Briefly, cells were treated with EdU at a dilution of 1:1,000 for 2 h at 37°C. After 4% paraformaldehyde fixation and 0.1% triton-100 permeabilization, the Apollo staining solution was applied for 30 m in the dark before Hoechst 33342 staining. Images were taken in three randomly chosen fields using an Axio Observer (Zeiss, Oberkochen, Germany) microscope.

Transwell migration assay

Aliquots of 200 μL serum-free medium containing 1×10^4 cells were planted in the upper chamber of the Transwell chamber (Corning Inc., Corning, NY, USA) and 800 μL of complete culture medium without cells was added to the lower chamber. 24 h later, 0.1% crystal violet (#G1062; Solarbio, Beijing, China) was used to stain the migrated cells. The number of migrated cells was counted after picture imaging.

Immunofluorescence

Cells grown on glass coverslips were treated with sodium arsenite (#S7400; Sigma-Aldrich, St Louis, MO, USA) for the indicated time. After 4% PFA fixation, cells were permeabilized with 0.1% Triton X-100 and then blocked with goat serum working solution (#ZLI-9056; ZSGB-Bio, Beijing, China), followed by incubation of indicated primary antibodies overnight at 4°C. On the next day, the coverslips were incubated with a fluorescent second antibody (#A21429 or #A11034; ThermoFisher Scientific) for one hour at room temperature. Then the slides were mounted with ProLong Gold Antifade mountant (#P36970; ThermoFisher Scientific) after extensive wash with PBS. The images were captured by a confocal microscope (TCS SP8; Leica, Mannheim, Germany).

Statistical analysis

The code and parameters used in this investigation were analyzed as previously described.[21] All experimental procedures and assays were repeated at least three times. The graph data were reported as means ± standard deviation. Student's *t*-test or one-way analysis with Bonferroni's correction was used to determine the significance of differences between or among groups. R and the GraphPad Prism programs were used to generate data graphics, and *p*-values <0.05 were considered significant ($^*p<0.05$; $^{**}p<0.01$; $^{***}p<0.001$; ns, not significant).

Results

Differentially expressed SGGs in normal liver and HCC tissue

Principal component analysis found that 463 SGGs had expression profiles that were distinct in HCC compared with other cancer types such as breast cancer and lung adenocarcinoma (Fig. 1A), suggesting that they were specific to the carcinogenesis of HCC. To identify the distinct SGGs in HCC, a TCGA-HCC cohort including 50 normal liver samples and 374 HCC samples was analyzed, revealing 34 differential SGGs (Fig. 1B). Interestingly, only the expression of the *ADAMTS13* gene was decreased in HCC, whereas the remaining 33 genes were all upregulated (Fig. 1C and Supplementary Table 6). The results led us to wonder whether SGGs were prone to be highly expressed, which predisposed SG formation in HCC. To verify this hypothesis, the expression of the 463 SGGs in normal and HCC tissue was analyzed in another six HCC cohorts. Expectedly, the number of highly expressed SGGs was dramatically more than that of low-expression SGGs in each indicated HCC cohort, and this discrepancy was most pronounced in the TCGA-HCC cohort (Fig. 1D). Additionally, in this TCGA-HCC cohort, we observed 200 SGGs whose expression was significantly correlated with overall survival (OS), and 196 of them all exhibited a significant disadvantageous association between gene expression and OS (Supplementary Table 7). Taken together, the results implied that highly expressed SGGs promoted more SG formation in HCC which led to an unfavorable outcome in HCC patients.

Functional enrichment analysis of differentially expressed SGGs in HCC

To further understand the functions of the 34 differential SGGs listed above, GO and KEGG analyses were carried out in the TCGA-HCC cohort. GO analysis revealed 30 significantly enriched GO terms using the differential SGGs, including 10 biological processes, 10 cellular components, and 10 molecular functions (Fig. 2A). KEGG analysis found that the above differential SGGs were enriched in DNA replication, the cell cycle, and gap junctions (Fig. 2B).

To establish functional links among the differential SGGs, we constructed a protein-protein interaction (PPI) network with Cytoscape software. It was shown that *CDK1* as the hub gene connected 15 differential SGGs (Fig. 2C–D). The biological contribution of *CDK1* in HCC was investigated by carrying out a single-gene GSEA analysis. As shown in Figure 2E, in addition to a positive correlation with the cell cycle pathway, genes involved in RNA degradation were upregulated in the *CDK1* high-expression HCC group, which was consistent with the role of SGGs in mRNA degradation.[23]

Construction of a prognostic signature using SGGs

To evaluate the correlation of the 34 differential SGGs with the OS of HCC patients, univariate Cox regression analysis was performed in the TCGA-HCC cohort. Twenty-two differentially expressed SGGs were found to be significantly correlated with the OS of HCC patients (Fig. 3A). To accurately predict patient prognosis, we further constructed a prognostic signature using multivariate Cox analysis based on the above 22 genes. Interestingly, four SGGs, *KPNA2*, *MEX3A*, *WDR62*, and *SFN*, were recognized as potential independent risk variables with *p*-values <0.05 (Table 1). Then, using the expression of the risk genes and regression coefficients, a four-SGG-based risk signature was created. Patient risk scores were as 0.096×expression amount of *SFN*+0.677×expression amount of *KPNA2*-0.649×expression amount of *WDR62*+0.331×expression amount of *MEX3A.* TCGA-HCC patients were stratified by the median score into high-risk and low-risk groups. Kaplan-Meier survival curves (log-rank $p<0.001$) indicated that the high-risk group had a poor prognosis and the low-risk group had a favorable outcome (Fig. 3B). The expression of the four-SGG signature, risk score scattering, and patient survival in the high- and low-risk groups are shown in Figure 3C–E.

Prognostic prediction power of the four-SGG signature

The association between various clinical features and OS was

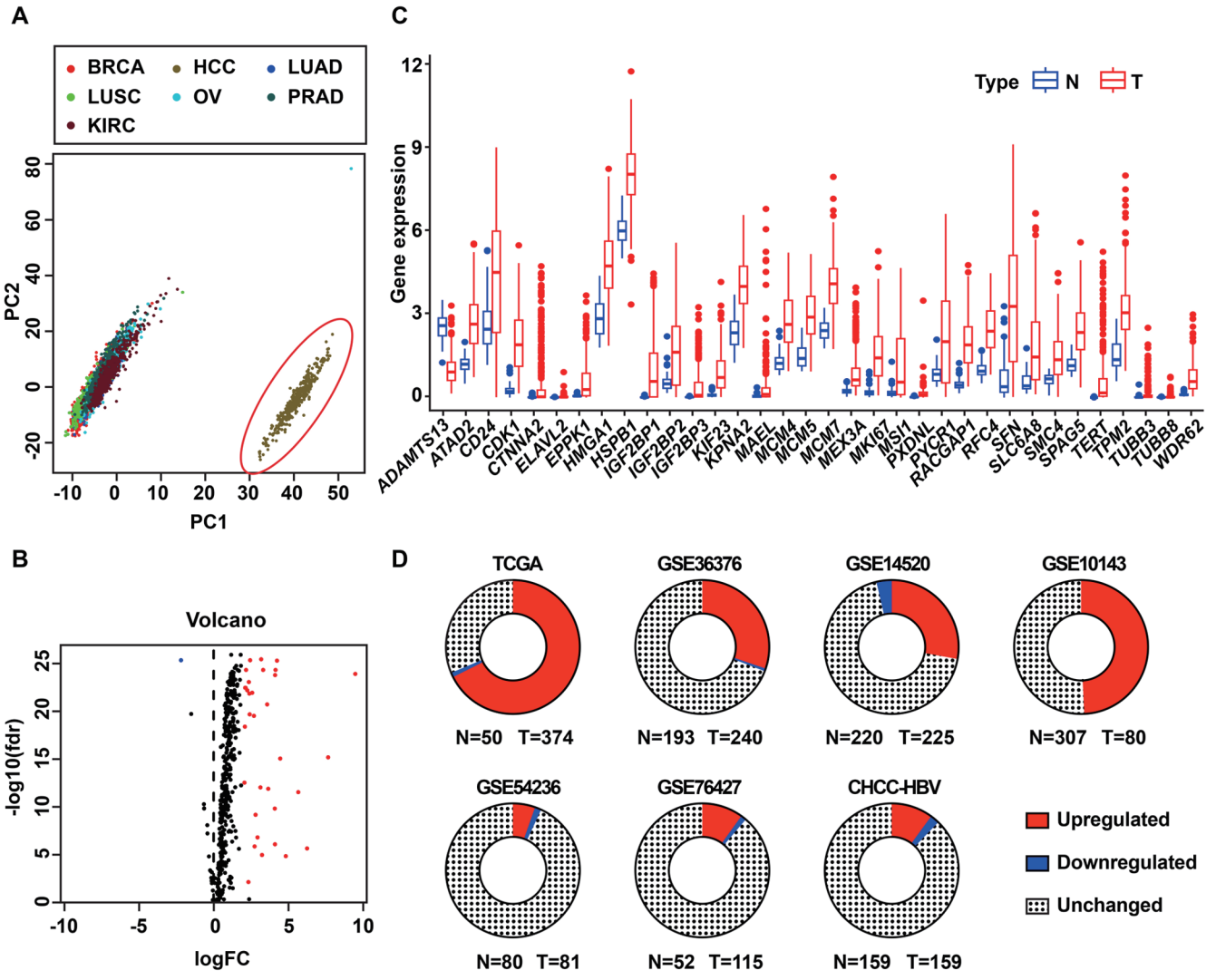

Fig. 1. Differentially expressed SGGs between HCC and normal liver tissue in TCGA-HCC cohort. (A) Principal component analysis of 463 SGGs. (B) Volcano plot of differentially expressed SGGs between HCC and normal liver tissue. Red marks indicate the overexpressed genes, whereas blue marks represent the low-expressed genes. (C) The 34 SGGs expression levels between normal and HCC groups. (D) Differential expressions of SGGs were respectively analyzed in different HCC cohorts. BRCA, breast cancer; HCC, hepatocellular carcinoma; KIRC, kidney renal clear cell carcinoma; LIHC, human liver hepatocellular carcinoma; LUAD, lung adenocarcinoma; LUSC, lung squamous cell carcinoma; N, normal liver sample; OV, ovarian serous cystadenocarcinoma; PRAD, prostate adenocarcinoma; SGGs, stress granule genes; T, HCC sample.

further examined by univariate and multivariate regression analysis. Univariate regression analysis showed that risk score, pathological stage, and, T stage were significantly associated with the OS of HCC patients (Fig. 4A). However, multivariate Cox regression analysis found that only the risk score was significantly associated (Fig. 4B).

To assess the efficacy of the SGG signature-based prognostic method, ROC curves were built. As shown in Fig. 4C, the risk score had a greater area under the curve (AUC, 0.776) than any of other clinical parameters, implying that it had the best performance of the constructed SGG model to predict the OS of HCC patients. To investigate the hidden explanation for this good performance of the four-SGG signature, the correlations of the expression of the four SGGs and HCC clinic characteristics were evaluated. As shown in Figure 4D and Supplementary Figure 1, the expression of *KPNA2*, *MEX3A*, and *WDR62* but not *SFN* were positively correlated with pathological stage, T stage, and tumor grade, even though all four genes were upregulated in HCC (Supplementary Fig. 2).[24] Kaplan-Meier survival analysis found that all four SGGs individually indicated poor OS and disease-free survival of HCC patients (Supplementary Fig. 3), which further explained the reliability of the four-SGG signature-dependent prognosis.

Validation of the four-SGG signature performance in the testing group

We further validated the effectiveness of the four-SGG signature in another HCC cohort from the ICGC database.[25] After stratifying 203 HCC patients into high- and low-risk groups based on the median risk score, we found that patients in low-risk groups had longer OS than those in high-risk groups (Supplementary Fig. 4A). Risk score scattering, patient survival condition, and four-SGG signature expression in both

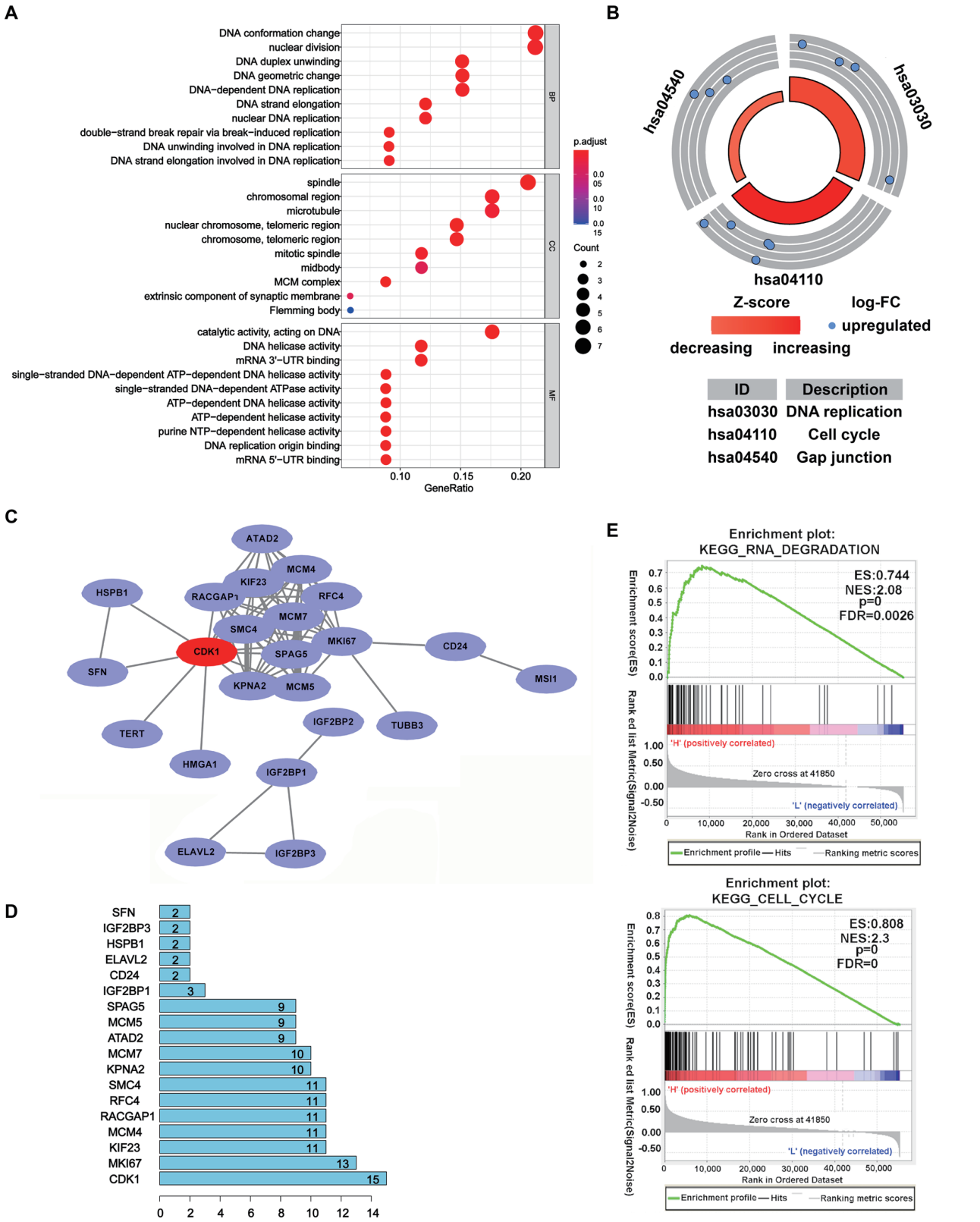

Fig. 2. Functional analysis of the distinct SGGs. (A) Gene ontology analysis of distinctly expressed SGGs. (B) KEGG analysis of distinctly expressed SGGs. (C) PPI networks of distinctly expressed SGGs were created by Cytoscape software. (D) *CDK1* is identified as the central gene among 34 differentially expressed SGGs. (E) *CDK1* GSEA analysis in the TCGA-HCC cohort. GSEA, gene set enrichment analysis; KEGG, kyoto encyclopedia of genes and genomes; PPI, protein-protein interaction.

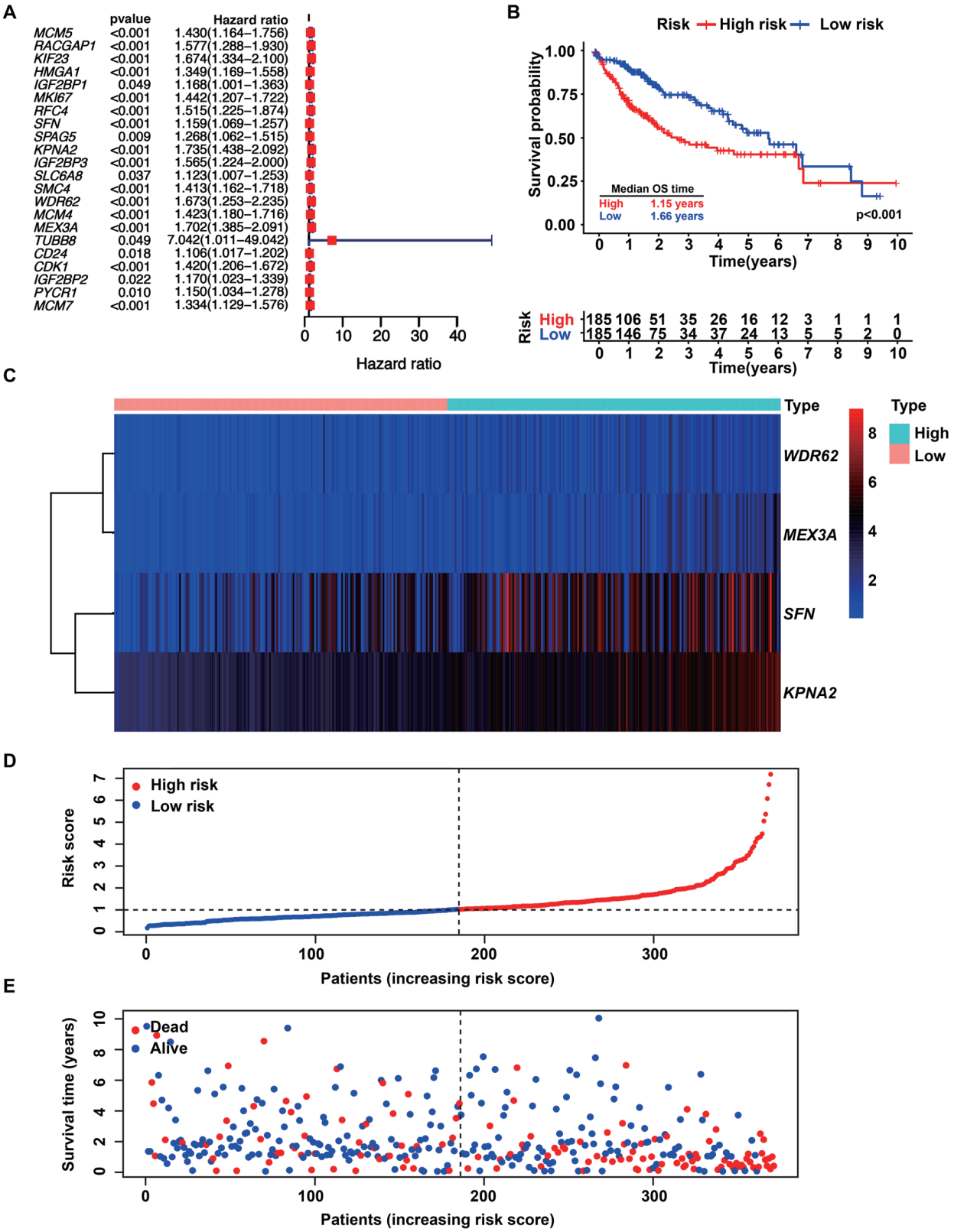

Fig. 3. Four-SGG signature identification in TCGA-HCC cohort. (A) Univariate Cox proportional hazards regression examination of the distinct SGGs in the TCGA-HCC cohort. (B) Kaplan-Meier evaluation of the OS using the four-SGG signature. High- and low-risk individuals with HCC are distributed utilizing the median risk score. (C) Four-SGG signature expression level in the low or high-risk group. (D, E) Scattering of risk scores and survival status for subjects in high- and low-risk groups. OS, overall survival.

Table 1. Regression coefficients of the potential independent risk genes

ID	Coefficient	HR	HR. 95L	HR. 95H	*p*-value
SFN	0.096	1.101	1.007	1.203	0.035
KPNA	0.677	1.968	1.438	2.694	<0.001
WDR62	−0.649	0.522	0.308	0.884	0.016
MEX3A	0.331	1.393	1.086	1.786	0.009

HR, hazard ratio.

groups are shown in Supplementary Figure 4B–D. The results confirmed the robust effectiveness of the four-SGG signature for predicting HCC prognosis.

Highly expressed KPNA2, MEX3A, WDR62, and SFN were involved in HCC development

Considering the strong prognostic power of the four-SGG signature in HCC, we wanted to experimentally validate whether these four proteins were involved in HCC development. To do this, the expression level of the genes was determined in HCC tissue and adjacent normal liver tissue. As shown in Figure 5A–C, compared with matched adjacent normal tissues, *KPNA2*, *MEX3A*, *WDR62*, and *SFN* were all significantly upregulated in HCC tissue both at the mRNA and protein levels. Expectedly, *KPNA2*, *MEX3A*, and *WDR62* were predominantly overexpressed in several HCC cell lines including Huh-7, Hep3B, HepG2, SK-Hep1, and PLC compared with L-02 normal human liver cells (Fig. 5D–E and Supplementary Fig. 5A). It was noted that the *SFN* expression pattern in HCC cell lines was not consistent with its expression in HCC tissues. This discordance was likely because of differences between HCC cell lines and HCC tumors.[26]

To further prove the oncogenic potential of these four genes in HCC, we first individually knocked them down in Hep3B and Huh7 cells (Fig. 6A–C and Supplementary Fig. 5B). It was then demonstrated that absence of *KPNA2*, *MEX3A*, *WDR62*, or *SFN* expression significantly impaired cell proliferation as documented by the CCK8 assay (Fig. 6D and Supplementary Fig. 5C), colony formation assay (Fig. 6E and Supplementary Fig. 5D), EdU staining (Fig. 6F). In addition, the Transwell migration assays showed that the migratory capacity of HCC cells was significantly weakened by *KPNA2*, *MEX3A*, *WDR62*, or *SFN* silencing (Fig. 6G). Overall, the results showed that high expression of *KPNA2*, *MEX3A*, *WDR62*, and *SFN* contributed to the proliferation and migration of HCC cells.

KPNA2, WDR62, MEX3A, and SFN contribute to HCC development dependent on their involvement in SG regulation

SG formation could be regarded as a protective mechanism for tumors against harsh environments such as hypoxia, acidity, and reactive oxygen species.[4] As SGs are promoted *in vitro* by sodium arsenite, which induces oxidative stress, and protein misfolding,[27] we next asked whether KPNA2, MEX3A, WDR62, and SFN were recruited to SGs and involved in their formation. To test this hypothesis, we first used the SG marker, G3BP1,[28] to establish a cell line that stably expressed G3BP1-GFP, Hep3B-G3BP1. As shown in Figure 7A and Supplementary Figure 6, sodium arsenite-induced G3BP1 puncta with optimal condition of 500 μM arsenite for 30 m without affecting cell viability. Interestingly, KPNA2, MEX3A, and WDR62, but not SFN appeared in these large SG foci at the same time. More significantly, after *KPNA2*, *MEX3A*, *WDR62*, or *SFN* were knocked down in Hep3B-G3BP1 cells, arsenite treatment failed to induce SG puncta in any of those cells compared with normal GFP-G3BP1-expressing cells. (Fig. 7B–C). The underlying mechanism might be the favorable role of these four proteins on *G3BP1* mRNA stability, as their depletion significantly reduced *G3BP1* mRNA expression (Fig. 7D).

SG participates in a wide variety of signaling pathways controlling cancer cell proliferation and invasion.[29] Therefore, it was expected that the knockdown of G3BP1 from SGs would disrupt their fundamental structure and weaken their tumor-promoting activity. In line with this, *G3BP1* knockdown (Supplementary Figs. 7A–B and 8A–B) not only significantly decreased SG formation under arsenic stress conditions (Supplementary Figs. 7C and 8C) but also significantly inhibited HCC cell proliferation and migration (Supplementary Figs. 7D–E and 8D–E). Collectively, the results revealed that KPNA2, MEX3A, WDR62, and SFN had protumorigenic activity through regulation of G3BP1-dependent SG formation.

Discussion

SGs are intracellular compartments formed in response to disadvantageous factors, and the pathogenesis of several diseases including cancer is associated with aberrantly active SG formations.[29] Several key tumorigenic drivers, such as mTOR, HDAC6, and *RAS* oncogene have been shown to promote SG formation.[5] The evidence shows that SGs function to orchestrate various oncogenic signals and external stimuli to mediate cancer cell proliferation, invasion, and metastasis. Therefore, it can be expected that SGs might be a promising prognostic and therapeutic target for cancer. To date, many SG-associated proteins have been identified, but no studies have used SGGs as a marker of clinical outcomes of HCC patients. Because we found the vast majority of SGGs were upregulated and associated with poor prognosis in HCC, it was interesting to investigate whether SGG-based methods acted as an independent prognostic tool to accurately predict the outcomes of HCC.

We found that 34 of 463 SGGs were differentially expressed in TCGA-HCC cohorts with a threshold of |log2 (FC)|>2. Surprisingly, only one differentially expressed gene was downregulated, and the remaining 33 were upregulated. We analyzed the expression pattern of the 463 SGGs in six other HCC cohorts and observed that many more differentially expressed SGGs were upregulated, which was similar to the findings in the TCGA-HCC cohort. To discover biomarkers of HCC prognosis, Cox regression models were applied for survival analysis in this study. Survival analysis is used to analyze the length of time between a start point (e.g., the detection of cancer) and an endpoint (e.g., mortality).[30] The effects of predictor variables such as age, sex, and tumor stage on the occurrence of a specific event such as death can be evaluated by Cox regression analysis.[31] Univariate Cox regression analysis evaluates the association of single factors with patient survival. Multivariate Cox regression simultaneously evaluates the effects of different factors on patient survival. Hazard ratios (HRs) reflect the probability

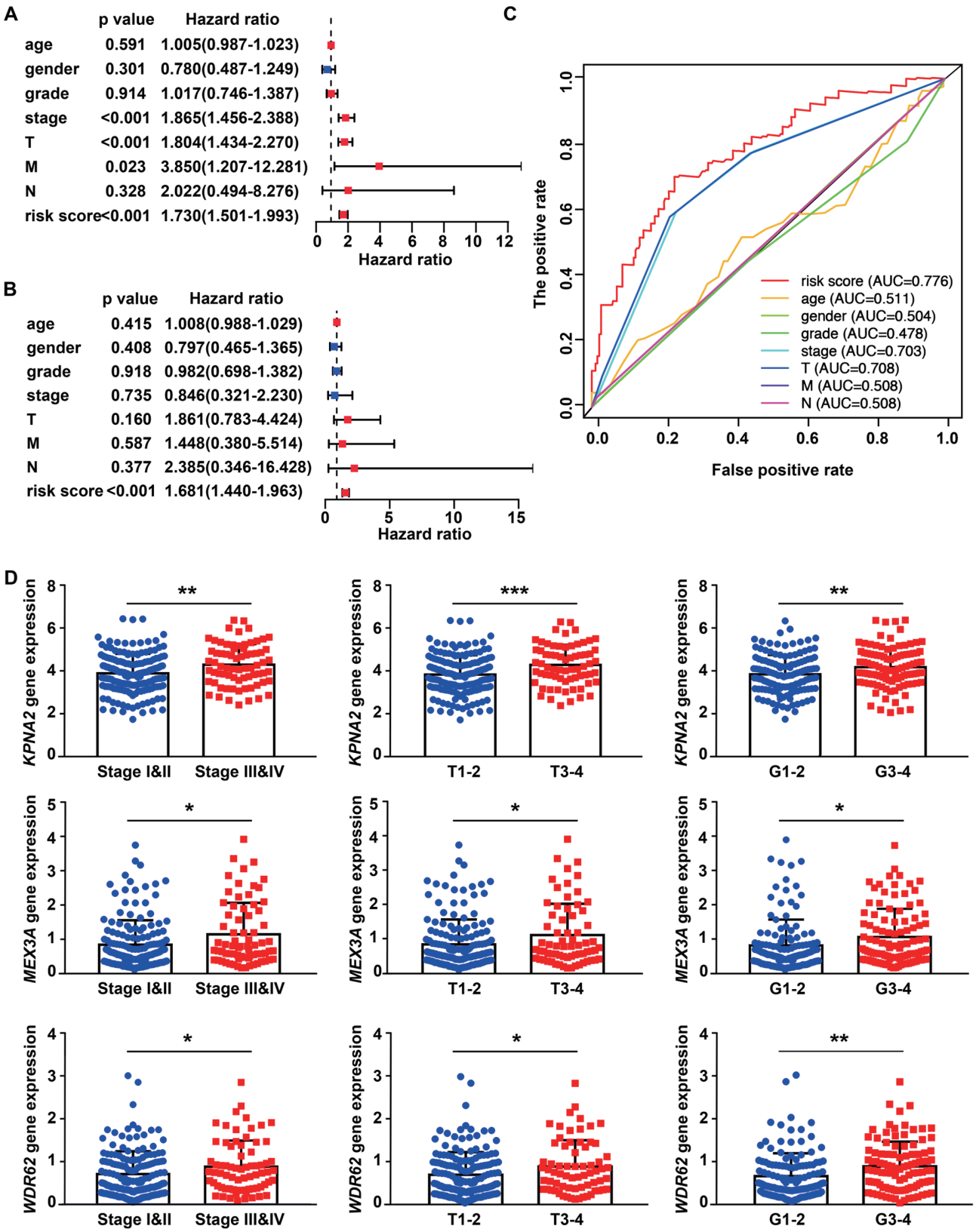

Fig. 4. Verification of the performance of the four-SGG signature in TCGA-HCC. (A) Univariate Cox regression tests. (B) Multivariate Cox regression tests. (C) Multi-index of ROC curve. (D) *KPNA2*, *WDR62*, and *MEX3A* gene expression levels in different pathological and T stages. ROC, receiver operating characteristic.

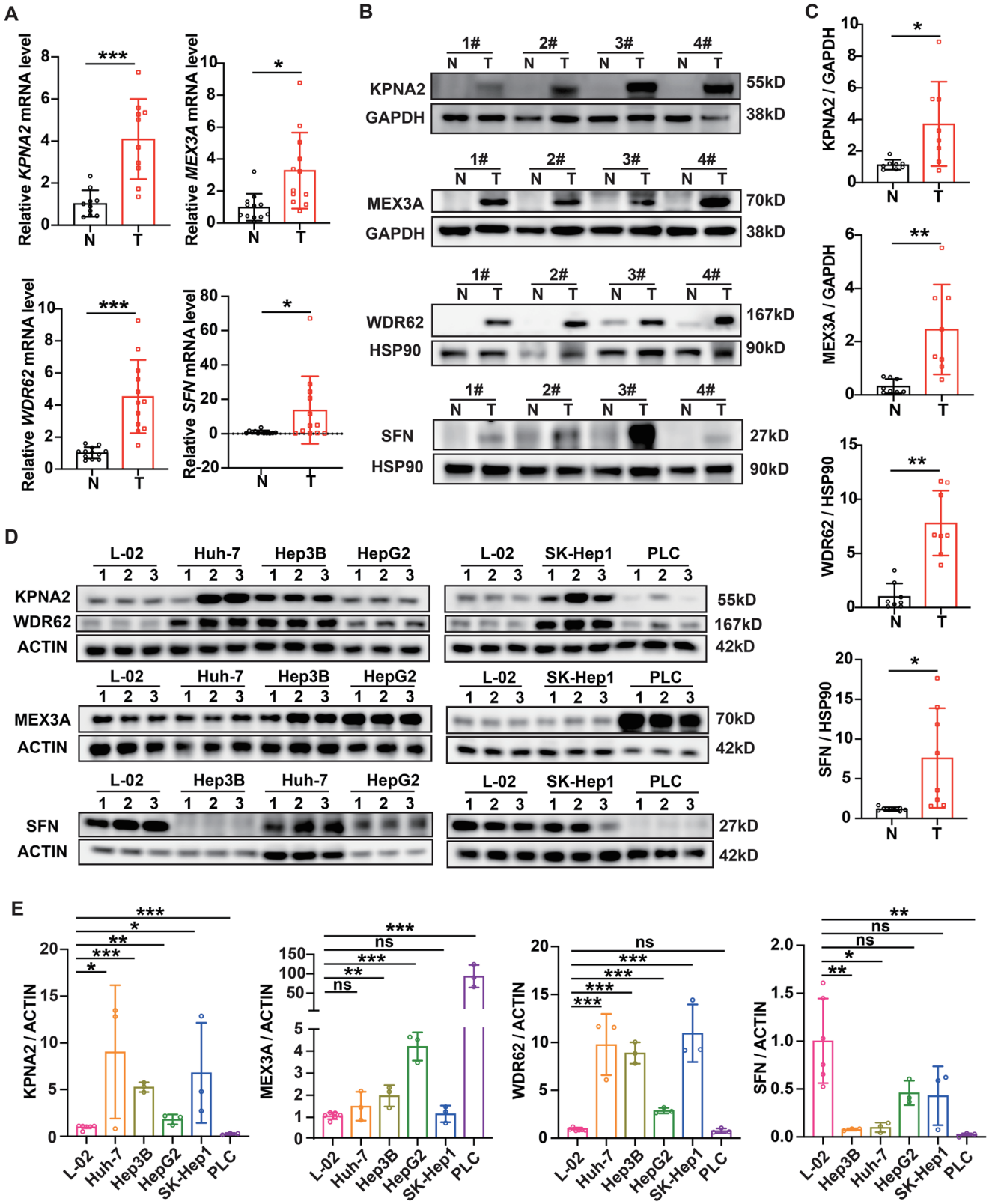

Fig. 5. *KPNA2*, *MEX3A*, *WDR62*, and *SFN* were upregulated in human HCC tissues and hepatoma cell lines. (A, B) mRNA levels (A) and protein levels (B) of *KPNA2*, *MEX3A*, *WDR62*, and *SFN* in hepatocellular carcinoma tissues (T) and neighboring healthy tissues (N). (C) Statistical analysis of (B). (D) KPNA2, MEX3A, WDR62, and SFN protein levels in the human healthy liver L-02 cell line and various human hepatoma cell lines. (E) Statistical analysis of (D).

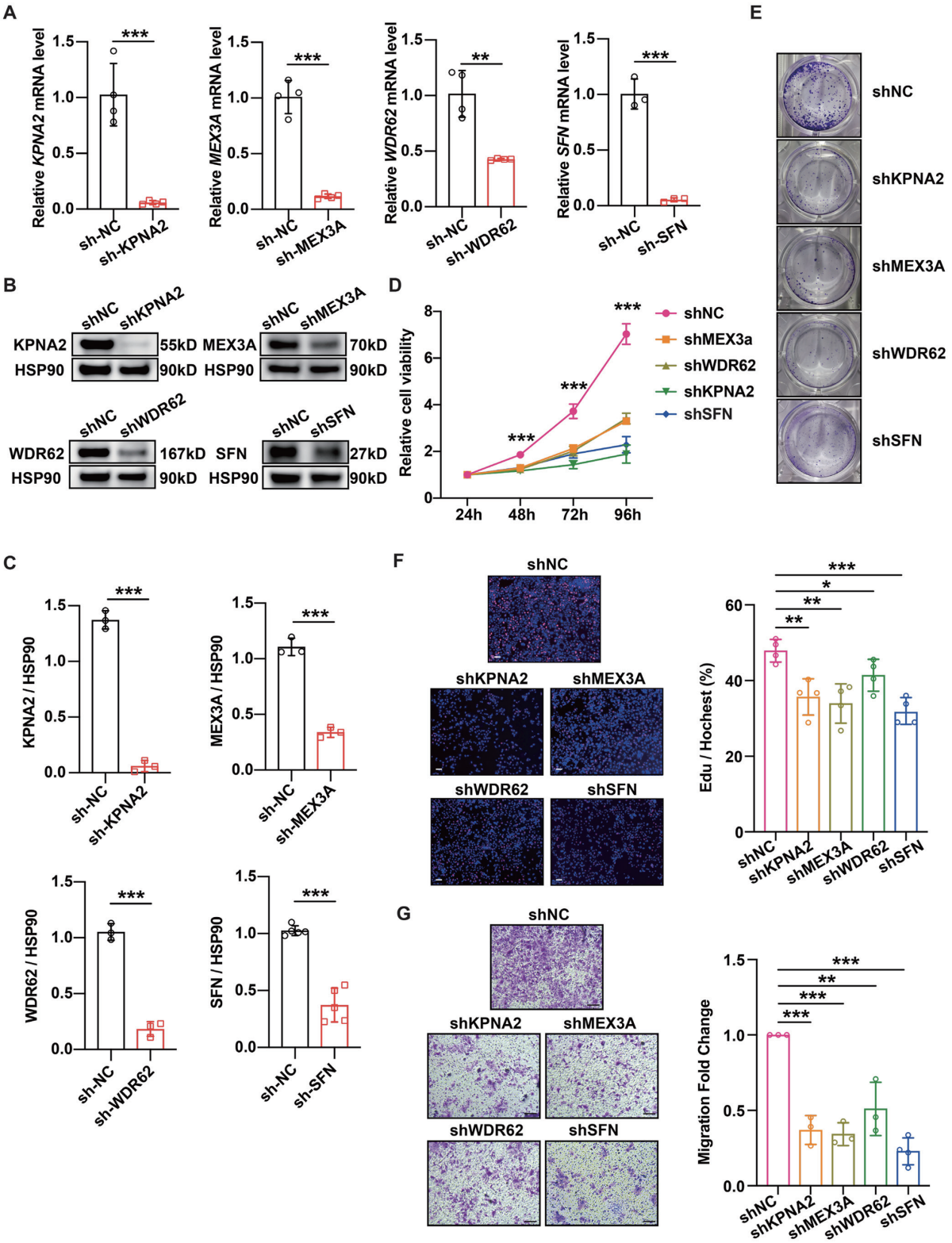

Fig. 6. *KPNA2*, *MEX3A*, *WDR62*, and *SFN* knockdown mitigated cell proliferation and migration. (A–C) The efficiency of the lentivirus-mediated shRNA knockdown of *KPNA2*, *MEX3A*, *WDR62*, and *SFN* expression in Hep3B, was verified both in mRNA (A) and protein levels (B and C). (D) The impacts of *KPNA2*, *MEX3A*, *WDR62*, and *SFN* deletion on Hep3B cell growth were evaluated by CCK8 assay. (E) Colony formation assays were conducted in Hep3B cells after *KPNA2*, *MEX3A*, *WDR62*, or *SFN* knockdown. (F) EdU assay was performed in Hep3B cells after *KPNA2*, *MEX3A*, *WDR62*, or *SFN* knockdown. Scale bar, 100 μm. (G) Cell migration was examined using Transwell assays after *KPNA2*, *MEX3A*, *WDR62*, or *SFN* knockdown in Hep3B cells. Scale bar, 100 μm.

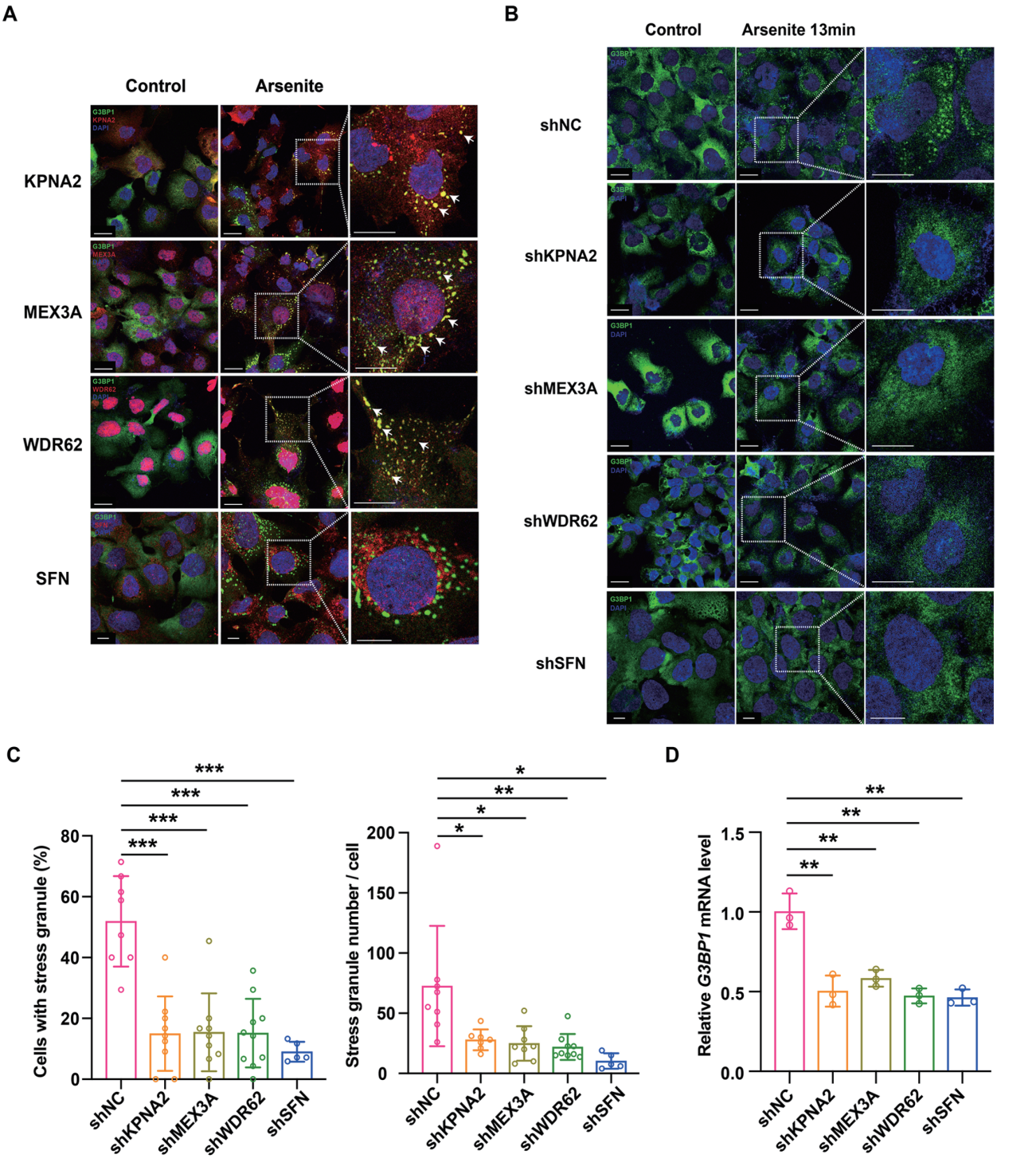

Fig. 7. The effect of *KPNA2*, *MEX3A*, *WDR62*, or *SFN* knockdown on SG assembly. (A) Colocalization analysis between G3BP1 and KPNA2, MEX3A, WDR62, or SFN in Hep3B cells. Arrows indicate merged sites. Scale bar, 25 μm. (B) Confocal analysis of stress granule formation after knocking down of *KPNA2*, *MEX3A*, *WDR62*, or *SFN* in Hep3B cells. Scale bar, 25 μm. (C) Statistical analysis of (B). The proportion of cells with SGs (left panel) and counts of SGs per cell (right panel). (D) *G3BP1* mRNA amounts were examined after individually knocking down of *KPNA2*, *MEX3A*, *WDR62*, or *SFN* in Hep3B cells. SGs, stress granules.

of a particular event such as death associated with specific predictor variable(s) over time.[30] Following univariate Cox regression and multivariate Cox regression analyses, a four-SGG signature consisting of KPNA2, MEX3A, WDR62, and SFN was established using data extracted from the TCGA-HCC cohort. The performance of our signature in prognostic prediction was further validated in another HCC cohort, which further demonstrated its effectiveness and reliability.

Because the deterioration of liver function contributes to poor HCC outcomes, in addition to gene expression-based predictive indexes, clinical indexes reflecting liver function, such as bilirubin, albumin, and alkaline phosphatase levels have also been reported to be independent biomarkers for HCC prognosis.[32,33] Thus, the integrative evaluation of gene expression and biochemical parameter-based predictive methods would be more precise in HCC prognosis.

Through binding to the target protein nuclear localization signal, KPNA2 was initially thought to mediate protein nucleus importation. Later, it was found to be localized in SGs and involved in SG assembly.[34] KPNA2 is highly expressed in various tumors and has tumor-promoting activity mediated by nuclear transport of cancer-associated cargo proteins such as c-Myc, PLAG1, and SMARCC1.[35] The oncogenic function of KPNA2 relating to SG formation demonstrated by us provides an alternative mechanism to explain its tumorigenic activity. WDR62 is localized in the nucleus and high expression in prostate and gastric cancer has been associated with decreased patient survival time.[36,37] Although WDR62 was reported to be recruited to SGs to promote JNK activation, whether it participated in SG formation has not been assessed because of technological limitations.[38] Consistent with previous findings, we detected recruitment of WDR62 to SGs; but found that WDR62 was required for SG assembly probably by stabilization of *G3BP1* mRNA. We also found for the first time that WDR62 was upregulated and served as a diagnostic marker in HCC. MEX3A, an RNA-binding protein, is overexpressed in multiple cancers like pancreatic, breast, and lung.[39] It was reported to promote cancer proliferation by stabilizing *CDK6* or *LAMA2* mRNA.[40] Bioinformatic analysis and experimental validation confirmed that MEX3A was overexpressed in HCC. It was also detected in SG and was required for SG formation, which provides another novel explanation of its oncogenic activity. As a member of the 14-3-3 family, SFN participates in diverse cellular activities such as protein stability, mitotic translation, and cell death.[41] Similar to our results, SFN expression was previously found to be increased in HCC and to have predictive accuracy when used in HCC diagnostics.[42] However, pathogenic mechanisms of SFN in HCC were not explored in those studies. Although SFN has already been defined as a component of SG by SG purification and proteomic analysis,[43] our results did not detect colocalization of SFN and SGs. Interestingly, the formation of SGs was still significantly attenuated after silencing SFN expression. The observed SG formation defects could account for the downregulation of the *G3BP1* in mRNA levels, with a similar reason for the effects of *KPNA2*, *MEX3A*, and *WDR62* knocking down on SG formation. Given the pivotal role of *G3BP1* in SGs, the detailed molecular mechanisms underlying these four SGGs in *G3BP1* regulation require further investigations.

The clinical information summarized from different datasets used in this research (Supplementary Table 8) corroborates the finding that more than 90% of HCC appears in patients with cirrhosis, which is attributed to various chronic liver diseases such as chronic hepatitis B virus (HBV) or hepatitis C virus (HCV) infection, alcohol abuse, and fatty liver disease.[44] These different HCC etiologies are associated with distinct genetic alterations or gene expression modulations that contribute to HCC development.[45,46] For example, TP53 and ACVR2V, two tumor suppressors, are most frequently mutated in HBV and NASH-related HCC, respectively.[45,47] Moreover, substantial differences in hepatocarcinogenesis have been observed in HBV and HCV-infected HCC.[48] It has often been reported that NASH-HCC or NAFLD-HCC, have unique molecular features that drive HCC progression.[47,49] The results support the view that HCC is a highly heterogeneous disorder with complex etiologies, and HCC without any chronic liver diseases is rare in the clinic.[50] Therefore, defining the intrinsically oncogenic mechanisms of HCC, which is not ascribed to any risk factors, is not easily evaluated in practice. An alternative approach to finding unique HCC-related genes was likely to compare tumor and adjacent liver tissues from HCC patients with specific chronic liver diseases such as HBV infection or NAFLD. TCGA database, well-known for its comprehensive cancer information worldwide, is widely used in gene expression and prognostic analysis. Although the TCGA-HCC cohort has a relatively large sample size (n=374), the different pathological types make the sample number in each pathological classification relatively small, which is not conducive to subsequent biomarker analysis under the specific etiologic condition. Therefore, many gene expression-based HCC prognosis studies frequently analyze the differences between HCC and noncancer samples without pathological classification in advance when adopting the TCGA-HCC database; after verification in another HCC cohort, the reliability and accuracy of these prognostic gene signatures for HCC could be conclusively determined.[17,51]

In this study, using similar strategies, we developed a four-SG-related gene signature in HCC prognosis and progression. The study has several limitations. First, the sample size was not large enough owing to resource limitations that may limit the generalization of our results. Second, information such as tumor etiologies, causes of death, and baseline clinical characteristics was lacking in the available datasets. That limited subgroup analysis based on different clinical features. An HCC database with a larger sample size, detailed clinical information, and specific etiologies should be used to investigate SGG-related HCC prognostic signatures, which might facilitate the establishment of more precise prognosis biomarkers suitable for particular HCC subtypes.

Conclusion

We established a four-SGG signature that accurately predicted survival outcomes of HCC patients. All four genes facilitated SG formation that contributed to HCC development. To our knowledge, this is the first study to decipher the molecular mechanisms underlying a predictive signature in HCC by the combination of bioinformatic analysis and experimental validation. This novel SGG signature might assist in the clinical diagnosis and treatment of HCC.

Funding

This research was funded by the National Natural Science Foundation of China (32200557 to DW), the "Outstanding University Driven by Talents" Program and Academic Promotion Program of Shandong First Medical University (2019LJ007 to JZ), the Natural Science Foundation of Shandong Province (ZR2022QH271 to DW), and the Postdoctoral Innovative Projects of Shandong Province (SDCX-ZG-202203047 to DW).

Conflict of interest

The authors have no conflict of interests related to this publication.

Author contributions

Study concept and design (DW, JZ), acquisition of data (DW, XF), analysis and interpretation of data (DW, ML, XF), drafting of the manuscript (DW, ML), critical revision of the manu-

script for important intellectual content (DW, JZ), generation of the tables and figures (DW, ML), and study supervision (DW, JZ). All authors have contributed significantly to this study and approved the final manuscript.

Ethical statement

All experiments involving human tissues were approved and supervised by the Medical Ethics Committee of Shandong Provincial Hospital Affiliated to Shandong First Medical University (approval number: SWYX: NO. 2019-202.) according to the latest version of the Declaration of Helsinki. Informed consent was obtained from all participants.

Data sharing statement

Data supporting the findings of this study are included in the supplementary information files.

References

[1] Guillén-Boixet J, Kopach A, Holehouse AS, Wittmann S, Jahnel M, Schlüßler R, *et al*. RNA-Induced Conformational Switching and Clustering of G3BP Drive Stress Granule Assembly by Condensation. Cell 2020;181(2):346–361.e17. doi:10.1016/j.cell.2020.03.049, PMID:32302572.

[2] Wang J, Gan Y, Cao J, Dong X, Ouyang W. Pathophysiology of stress granules: An emerging link to diseases (Review). Int J Mol Med 2022;49(4):44. doi:10.3892/ijmm.2022.5099, PMID:35137915.

[3] Chen X, Cubillos-Ruiz JR. Endoplasmic reticulum stress signals in the tumour and its microenvironment. Nat Rev Cancer 2021;21(2):71–88. doi:10.1038/s41568-020-00312-2, PMID:33214692.

[4] Gao X, Jiang L, Gong Y, Chen X, Ying M, Zhu H, *et al*. Stress granule: A promising target for cancer treatment. Br J Pharmacol 2019;176(23):4421–4433. doi:10.1111/bph.14790, PMID:31301065.

[5] Song MS, Grabocka E. Stress Granules in Cancer. Rev Physiol Biochem Pharmacol 2023;185:25–52. doi:10.1007/112_2020_37, PMID:32789791.

[6] Nunes C, Mestre I, Marcelo A, Koppenol R, Matos CA, Nóbrega C. MSGP: the first database of the protein components of the mammalian stress granules. Database (Oxford) 2019;2019:baz031. doi:10.1093/database/baz031, PMID:30820574.

[7] Tourrière H, Chebli K, Zekri L, Courselaud B, Blanchard JM, Bertrand E, *et al*. The RasGAP-associated endoribonuclease G3BP assembles stress granules. J Cell Biol 2003;160(6):823–831. doi:10.1083/jcb.200212128, PMID:12642610.

[8] Alam U, Kennedy D. Rasputin a decade on and more promiscuous than ever? A review of G3BPs. Biochim Biophys Acta Mol Cell Res 2019;1866(3):360–370. doi:10.1016/j.bbamcr.2018.09.001, PMID:30595162.

[9] Somasekharan SP, El-Naggar A, Leprivier G, Cheng H, Hajee S, Grunewald TG, *et al*. YB-1 regulates stress granule formation and tumor progression by translationally activating G3BP1. J Cell Biol 2015;208(7):913–929. doi:10.1083/jcb.201411047, PMID:25800057.

[10] Wang Y, Fu D, Chen Y, Su J, Wang Y, Li X, *et al*. G3BP1 promotes tumor progression and metastasis through IL-6/G3BP1/STAT3 signaling axis in renal cell carcinomas. Cell Death Dis 2018;9(5):501. doi:10.1038/s41419-018-0504-2, PMID:29717134.

[11] Bray F, Ferlay J, Soerjomataram I, Siegel RL, Torre LA, Jemal A. Global cancer statistics 2018: GLOBOCAN estimates of incidence and mortality worldwide for 36 cancers in 185 countries. CA Cancer J Clin 2018;68(6):394–424. doi:10.3322/caac.21492, PMID:30207593.

[12] Gunasekaran G, Bekki Y, Lourdusamy V, Schwartz M. Surgical Treatments of Hepatobiliary Cancers. Hepatology 2021;73(Suppl 1):128–136. doi:10.1002/hep.31325, PMID:32438491.

[13] Cheng AL, Kang YK, Chen Z, Tsao CJ, Qin S, Kim JS, *et al*. Efficacy and safety of sorafenib in patients in the Asia-Pacific region with advanced hepatocellular carcinoma: a phase III randomised, double-blind, placebo-controlled trial. Lancet Oncol 2009;10(1):25–34. doi:10.1016/S1470-2045(08)70285-7, PMID:19095497.

[14] Kim TH, Kim SY, Tang A, Lee JM. Comparison of international guidelines for noninvasive diagnosis of hepatocellular carcinoma: 2018 update. Clin Mol Hepatol 2019;25(3):245–263. doi:10.3350/cmh.2018.0090, PMID:30759967.

[15] Fu J, Wang H. Precision diagnosis and treatment of liver cancer in China. Cancer Lett 2018;412:283–288. doi:10.1016/j.canlet.2017.10.008, PMID:29050983.

[16] Forner A, Llovet JM, Bruix J. Hepatocellular carcinoma. Lancet 2012;379(9822):1245–1255. doi:10.1016/s0140-6736(11)61347-0, PMID:22353262.

[17] Wan S, Lei Y, Li M, Wu B. A prognostic model for hepatocellular carcinoma patients based on signature ferroptosis-related genes. Hepatol Int 2022;16(1):112–124. doi:10.1007/s12072-021-10248-w, PMID:34449009.

[18] Fang Q, Chen H. Development of a Novel Autophagy-Related Prognostic Signature and Nomogram for Hepatocellular Carcinoma. Front Oncol 2020;10:591356. doi:10.3389/fonc.2020.591356, PMID:33392087.

[19] Shi Q, Zhu Y, Ma J, Chang K, Ding D, Bai Y, *et al*. Prostate Cancer-associated SPOP mutations enhance cancer cell survival and docetaxel resistance by upregulating Caprin1-dependent stress granule assembly. Mol Cancer 2019;18(1):170. doi:10.1186/s12943-019-1096-x, PMID:31771591.

[20] Gao Q, Zhu H, Dong L, Shi W, Chen R, Song Z, *et al*. Integrated Proteogenomic Characterization of HBV-Related Hepatocellular Carcinoma. Cell 2019;179(2):561–577.e22. doi:10.1016/j.cell.2019.08.052, PMID:31585088.

[21] Wang D, Liu S, Wang G. Establishment of an Endocytosis-Related Prognostic Signature for Patients With Low-Grade Glioma. Front Genet 2021;12:709666. doi:10.3389/fgene.2021.709666, PMID:34552618.

[22] Hummon AB, Lim SR, Difilippantonio MJ, Ried T. Isolation and solubilization of proteins after TRIzol extraction of RNA and DNA from patient material following prolonged storage. Biotechniques 2007;42(4):467–472. doi:10.2144/000112401, PMID:17489233.

[23] Campos-Melo D, Hawley ZCE, Droppelmann CA, Strong MJ. The Integral Role of RNA in Stress Granule Formation and Function. Front Cell Dev Biol 2021;9:621779. doi:10.3389/fcell.2021.621779, PMID:34095105.

[24] Tang Z, Kang B, Li C, Chen T, Zhang Z. GEPIA2: an enhanced web server for large-scale expression profiling and interactive analysis. Nucleic Acids Res 2019;47(W1):W556–W560. doi:10.1093/nar/gkz430, PMID:31114875.

[25] Lian Q, Wang S, Zhang G, Wang D, Luo G, Tang J, *et al*. HCCDB: A Database of Hepatocellular Carcinoma Expression Atlas. Genomics Proteomics Bioinformatics 2018;16(4):269–275. doi:10.1016/j.gpb.2018.07.003, PMID:30266410.

[26] Chen B, Sirota M, Fan-Minogue H, Hadley D, Butte AJ. Relating hepatocellular carcinoma tumor samples and cell lines using gene expression data in translational research. BMC Med Genomics 2015;8:S5. doi:10.1186/1755-8794-8-S2-S5, PMID:26043652.

[27] Markmiller S, Fulzele A, Higgins R, Leonard M, Yeo GW, Bennett EJ. Active Protein Neddylation or Ubiquitylation Is Dispensable for Stress Granule Dynamics. Cell Rep 2019;27(5):1356–1363.e3. doi:10.1016/j.celrep.2019.04.015, PMID:31042464.

[28] Yang P, Mathieu C, Kolaitis RM, Zhang P, Messing J, Yurtsever U, *et al*. G3BP1 Is a Tunable Switch that Triggers Phase Separation to Assemble Stress Granules. Cell 2020;181(2):325–345.e28. doi:10.1016/j.cell.2020.03.046, PMID:32302571.

[29] Lavalée M, Curdy N, Laurent C, Fournié JJ, Franchini DM. Cancer cell adaptability: turning ribonucleoprotein granules into targets. Trends Cancer 2021;7(10):902–915. doi:10.1016/j.trecan.2021.05.006, PMID:34144941.

[30] Bradburn MJ, Clark TG, Love SB, Altman DG. Survival analysis part II: multivariate data analysis—an introduction to concepts and methods. Br J Cancer 2003;89(3):431–436. doi:10.1038/sj.bjc.6601119, PMID:12888808.

[31] George B, Seals S, Aban I. Survival analysis and regression models. J Nucl Cardiol 2014;21(4):686–694. doi:10.1007/s12350-014-9908-2, PMID:24810431.

[32] Johnson PJ, Berhane S, Kagebayashi C, Satomura S, Teng M, Reeves HL, *et al*. Assessment of liver function in patients with hepatocellular carcinoma: a new evidence-based approach-the ALBI grade. J Clin Oncol 2015;33(6):550–558. doi:10.1200/JCO.2014.57.9151, PMID:25512453.

[33] Li L, Mo F, Hui EP, Chan SL, Koh J, Tang NLS, *et al*. The association of liver function and quality of life of patients with liver cancer. BMC Gastroenterol 2019;19(1):66. doi:10.1186/s12876-019-0984-2, PMID:31046687.

[34] Fujimura K, Suzuki T, Yasuda Y, Murata M, Katahira J, Yoneda Y. Identification of importin alpha1 as a novel constituent of RNA stress granules. Biochim Biophys Acta 2010;1803(7):865–871. doi:10.1016/j.bbamcr.2010.03.020, PMID:20362631.

[35] Han Y, Wang X. The emerging roles of KPNA2 in cancer. Life Sci 2020;241:117140. doi:10.1016/j.lfs.2019.117140, PMID:31812670.

[36] Zeng S, Tao Y, Huang J, Zhang S, Shen L, Yang H, *et al*. WD40 repeat-containing 62 overexpression as a novel indicator of poor prognosis for human gastric cancer. Eur J Cancer 2013;49(17):3752–3762. doi:10.1016/j.ejca.2013.07.015, PMID:23920402.

[37] Das R, Sjöström M, Shrestha R, Yogodzinski C, Egusa EA, Chesner LN, *et al*. An integrated functional and clinical genomics approach reveals genes driving aggressive metastatic prostate cancer. Nat Commun 2021;12(1):4601. doi:10.1038/s41467-021-24919-7, PMID:34326322.

[38] Wasserman T, Katsenelson K, Daniliuc S, Hasin T, Choder M, Aronheim A. A novel c-Jun N-terminal kinase (JNK)-binding protein WDR62 is recruited to stress granules and mediates a nonclassical JNK activation. Mol Biol Cell 2010;21(1):117–130. doi:10.1091/mbc.e09-06-0512, PMID:19910486.

[39] Lederer M, Müller S, Glaß M, Bley N, Ihling C, Sinz A, *et al*. Oncogenic Potential of the Dual-Function Protein MEX3A. Biology (Basel) 2021;10(5):415. doi:10.3390/biology10050415, PMID:34067172.

[40] Liang J, Li H, Han J, Jiang J, Wang J, Li Y, *et al*. Mex3a interacts with LAMA2 to promote lung adenocarcinoma metastasis via PI3K/AKT pathway. Cell Death Dis 2020;11(8):614. doi:10.1038/s41419-020-02858-3, PMID:32792503.

[41] Lee MH, Lozano G. Regulation of the p53-MDM2 pathway by 14-3-3 sigma and other proteins. Semin Cancer Biol 2006;16(3):225–234. doi:10.1016/j.semcancer.2006.03.009, PMID:16697215.

[42] Zhang Y, Li Y, Lin C, Ding J, Liao G, Tang B. Aberrant upregulation of 14-3-3σ and EZH2 expression serves as an inferior prognostic biomarker for hepatocellular carcinoma. PLoS One 2014;9(9):e107251. doi:10.1371/journal.pone.0107251, PMID:25226601.

[43] Youn JY, Dunham WH, Hong SJ, Knight JDR, Bashkurov M, Chen GI, *et al*. High-Density Proximity Mapping Reveals the Subcellular Organization of mRNA-Associated Granules and Bodies. Mol Cell 2018;69(3):517–532.e11. doi:10.1016/j.molcel.2017.12.020, PMID:29395067.

[44] Llovet JM, Kelley RK, Villanueva A, Singal AG, Pikarsky E, Roayaie S, *et al*.

Hepatocellular carcinoma. Nat Rev Dis Primers 2021;7(1):6. doi:10.1038/s41572-020-00240-3, PMID:33479224.
[45] Amaddeo G, Cao Q, Ladeiro Y, Imbeaud S, Nault JC, Jaoui D, *et al*. Integration of tumour and viral genomic characterizations in HBV-related hepatocellular carcinomas. Gut 2015;64(5):820–829. doi:10.1136/gutjnl-2013-306228, PMID:25021421.
[46] Yang JD, Hainaut P, Gores GJ, Amadou A, Plymoth A, Roberts LR. A global view of hepatocellular carcinoma: trends, risk, prevention and management. Nat Rev Gastroenterol Hepatol 2019;16(10):589–604. doi:10.1038/s41575-019-0186-y, PMID:31439937.
[47] Pinyol R, Torrecilla S, Wang H, Montironi C, Piqué-Gili M, Torres-Martin M, *et al*. Molecular characterisation of hepatocellular carcinoma in patients with non-alcoholic steatohepatitis. J Hepatol 2021;75(4):865–878. doi:10.1016/j.jhep.2021.04.049, PMID:33992698.
[48] Sun S, Li Y, Han S, Jia H, Li X, Li X. A comprehensive genome-wide profiling comparison between HBV and HCV infected hepatocellular carcinoma. BMC Med Genomics 2019;12(1):147. doi:10.1186/s12920-019-0580-x, PMID:31660973.
[49] Wong AM, Ding X, Wong AM, Xu M, Zhang L, Leung HH, *et al*. Unique molecular characteristics of NAFLD-associated liver cancer accentuate β-catenin/TNFRSF19-mediated immune evasion. J Hepatol 2022;77(2):410–423. doi:10.1016/j.jhep.2022.03.015, PMID:35351523.
[50] Osyntsov A, Zemel M, Cohen N, Cooper JM, Krenawi M, Krayim B, *et al*. An Unusual Presentation of HCC in a Patient with No Underlying Liver Disease: A Case Study. Case Rep Oncol 2022;15(3):995–1000. doi:10.1159/000526929, PMID:36636683.
[51] Zhu G, Xia H, Tang Q, Bi F. An epithelial-mesenchymal transition-related 5-gene signature predicting the prognosis of hepatocellular carcinoma patients. Cancer Cell Int 2021;21(1):166. doi:10.1186/s12935-021-01864-5, PMID:33712026.